

Stellar Energy Loss Rates from Photoneutrino Process in Minimal Extension Standard Model

C. Aydın

Department of Physics, Karadeniz Technical University, 61080, Trabzon, Turkey

Abstract: Using the minimal extension of Standard Model taking into account the charge radius and the anapole moments of neutrino, we have derived analytic expressions for the stellar energy loss rates due to the production of the neutrino pair process $e^- + \gamma \rightarrow e^- + \nu_e + \bar{\nu}_e$ in a hot plasma for three limiting regimes (nondegenerate, intermediate and degenerate electrons) of temperature, the electron's chemical potential and plasma's energy. Obtained results show that there is approximately extra 10% contribution by using the considered calculations.

Key words: Neutrinos, Pair Production, Stellar Energy-Loss Rates, Form Factors, Electron-Positron Plasmas.

PACS:

1 Introduction

Energy loss due to neutrino emission is an important process astrophysical problems. Neutrinos are produced in stellar interiors, because of their interacting with stellar matter weakly, they can easily absorb energy that would otherwise take much longer to be transported to the surface by radiation or convection. The resulting energy sink in the center of the star can dictate the star's rate of nuclear burning, structure and evolution, and ultimately how its life ends. In this cases, if any process produce neutrino pairs, it is an extremely important energy-loss mechanism for stars in certain density and temperature ranges. The photoneutrino process were first studied by Ritus [1] and by Chiu and Stabler [2] for non-degenerated as well as degenerate electron in Fermi $V-A$ theory. Beaudet, Betrosian and Salpeter[3] provided analytic approximations for the photo-neutrino process in the same model. Dicus [4] recalculated this process in the framework of Standard Model(SM). He gave global correction factors to these rates to include neutral current effects. Schinder et al.[5] numerically recalculated the emission rates in SM and found good agreement with The BPS formulae together with the temperature range $10^{10} - 10^{11} K$. In 1989, Itoh et al.[6] whose improved on their previous work [7] provided an alternate set of approximation formulae on their previous work. All above studies, the photon is taken ordinary photon. As regards ordinary photon this process is supposed to play an important role for the low density $\rho/\mu_e = 10^5 gr/cm^3$ and comparatively low temperature $T = 4 \cdot 10^8 K$. These calculation has been done for about sixty years ago by many authors in $V-A$ model[1-3], SM [4-12] and magnetic model[13]. Dutta et al.[10, 11] considered instead of ordinary photon the massive photon (plasmon) and the angular dependence of the emitted neutrinos for this process in hot and dense matter. In prior their study didn't consider the energy and angular dependencies of the neutrinos in the calculations of the total energy lost rates, because they used Lenard's formula [14]. They presented numerical results for widely varying conditions of temperatures and density.

In recent studies, we have investigated the production neutrino pair process of the energy loss[15] and energy deposition rate for neutrino pair process [16]in the minimal extension standard model.Also,the photo-neutrino, plasmon and bremsstrahlung processes are the dominant cause of the stellar energy loss rates in different regions present within the density-temperature plane.These new calculations could contribute to a better understanding of the neutrino physics, and looking for new physics beyond standard model(SM).

In this study, we have investigated the energy loss rate of photo-neutrino pair annihilation process $e^- + \gamma \rightarrow e^- + \nu_e + \bar{\nu}_e$ in the extension SM includes neutrino electromagnetic form factors (especially charge radius and anapole moment) effect on neutrino photon interaction in to account the $\gamma\nu\bar{\nu}$ vertex for the Dirac neutrinos [15-31] in Section II. These effects not considered previously for this process in literature. In Section III, we present our the numerical results. This section also contain discussion and our conclusion.

Received XX Feb 2022

1) E-mail: coskun@ktu.edu.tr

2 Calculation

The Feynman diagrams for the process $e^-(p) + \gamma(k) \rightarrow e^-(p') + \nu_e(q_1) + \bar{\nu}_e(q_2)$ are shown in Figure 1. The symbols in the parentheses are the momenta of the particles.

After Fierz transformation, the matrix element of the process can be written in SM (Figure 1 (a)-(d)) in the low energy limit as

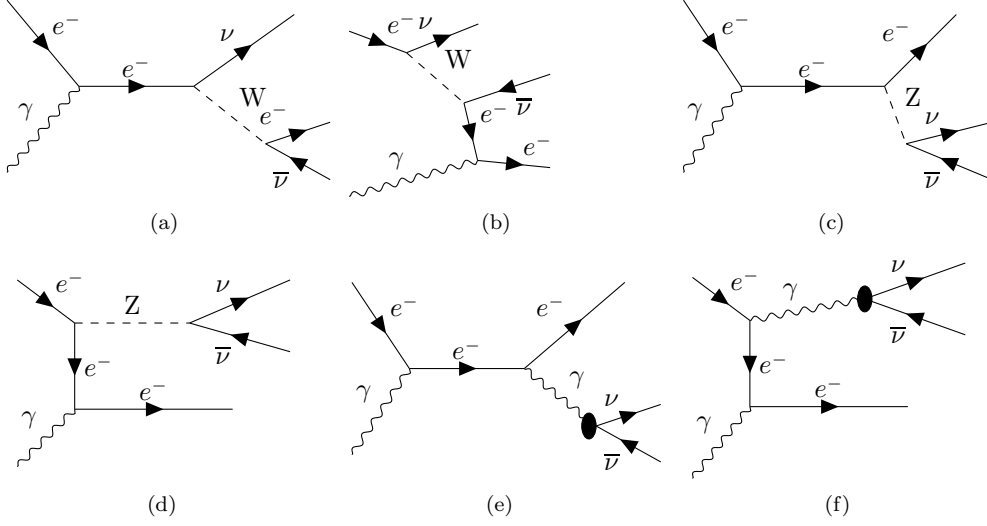


Fig. 1: The leading order Feynman diagrams for the photo-neutrino process. The black disk in (e and f) represents the interaction arising from effective neutrino interaction beyond the SM.

$$\begin{aligned} \mathcal{M}^{(SM)} &= -\frac{ieG_F}{\sqrt{2}} \left[\bar{u}_e(p') \gamma^\beta (C_V - C_A \gamma_5) \frac{(\not{p} + \not{k} + m_e)}{2pk + k^2} \not{\epsilon} u_e(p) + \bar{u}_e(p') \not{\epsilon} \frac{(\not{p}' - \not{k} + m_e)}{-2p'k + k^2} \gamma^\beta (C_V - C_A \gamma_5) u_e(p) \right] \\ &\times \bar{u}_\nu(q_1) \gamma_\beta (1 - \gamma_5) v_\nu(q_2) \end{aligned} \quad (1)$$

where u and v are Dirac spinors, $C_V = \frac{1}{2} + 2\sin^2\theta_W$ and $C_A = \frac{1}{2}$ for ν_e , and $C_V = -\frac{1}{2} + 2\sin^2\theta_W$ and $C_A = -\frac{1}{2}$ for ν_μ and ν_τ because the electron neutrinos interact with both W and Z bosons but the muon and tau neutrinos interact only with Z (see the case Figure 1 (c)-(d)). In this study, we restrict ourselves by considering only the electron neutrinos.

The matrix element of the (Figure 1 (e)-(f)) is given by

$$\mathcal{M}^{(\gamma)} = \mathcal{M}^{(Q)} + \mathcal{M}^{(\mu)} \quad (2)$$

where

$$\begin{aligned} \mathcal{M}^{(Q)} &= \frac{i4\pi\alpha}{q^2} \bar{u}_\nu(q_1) (\gamma^\beta - \frac{q^\beta \not{q}}{q^2}) \left[\frac{q^2}{6} \langle r_\nu^2 \rangle \right] v_\nu(q_2) \\ &\times (ie)^2 \left[\bar{u}_e(p') \gamma^\beta \frac{(\not{p} + \not{k} + m_e)}{2pk + k^2} \not{\epsilon} u_e(p) + \bar{u}_e(p') \not{\epsilon} \frac{(\not{p}' - \not{k} + m_e)}{-2p'k + k^2} \gamma^\beta u_e(p) \right] \end{aligned} \quad (3)$$

$$\begin{aligned} \mathcal{M}^{(\mu)} &= -i \frac{2\pi\alpha}{q^2} \bar{u}_\nu(q_1) \sigma^{\beta\lambda} q_\lambda [\mu] v_\nu(q_2) \\ &\times (ie)^2 \left[\bar{u}_e(p') \gamma^\beta \frac{(\not{p} + \not{k} + m_e)}{2pk + k^2} \not{\epsilon} u_e(p) + \bar{u}_e(p') \not{\epsilon} \frac{(\not{p}' - \not{k} + m_e)}{-2p'k + k^2} \gamma^\beta u_e(p) \right] \end{aligned} \quad (4)$$

where $q = q_1 + q_2$, $\alpha = e^2/4\pi$ is the fine structure constant, $\langle r_\nu^2 \rangle = \langle r^2 \rangle + 6\gamma_5 a$ is the mean charge radius of neutrino (in fact, it is the squared charge radius) and $\mu = \mu_\nu + i\gamma_5 d_\nu$ is the neutrino magnetic moment [15, 23].

The total matrix element of the process can be written as

$$\mathcal{M}_t = \mathcal{M}^{(SM)} + \mathcal{M}^{(Q)} + \mathcal{M}^{(\mu)}. \quad (5)$$

There is no interference between the helicity-conserving ($\mathcal{M}^{(SM)}$ and $\mathcal{M}^{(Q)}$) and helicity-flipping ($\mathcal{M}^{(\mu)}$) amplitudes. Combining the helicity-conserving amplitudes and using $q_\mu J^\mu(q) = 0$, we find

$$\begin{aligned} \mathcal{M}^{(SM)} + \mathcal{M}^{(Q)} &= \frac{i e G_F}{\sqrt{2}} \left[\bar{u}_e(p') \gamma^\beta (C'_V - C_A \gamma_5) \frac{(\not{p} + \not{k} + m_e)}{2pk + k^2} \not{\epsilon} u_e(p) + \bar{u}_e(p') \not{\epsilon} \frac{(\not{p}' - \not{k} + m_e)}{-2p'k + k^2} \gamma^\beta (C'_V - C_A \gamma_5) u_e(p) \right] \\ &\times \bar{u}_\nu(q_1) \gamma_\beta (1 - \gamma_5) v_\nu(q_2) \end{aligned} \quad (6)$$

where $C'_V = C_V + \frac{\sqrt{2}\pi\alpha}{3G_F} < r_\nu^2 > [15, 16, 18-21, 28, 30, 31]$. We neglect the helicity-flipping amplitudes because the contribution of the magnetic moment term ($\mathcal{M}^{(\mu)}$) is very small for $\mu_{\nu_e} \leq 10^{-12} \mu_B [32-35]$ or $\mu_{\nu_\tau} \leq 10^{-10} \mu_B [36]$.

Then the total matrix element square can be written as

$$|\mathcal{M}_t|^2 = |\mathcal{M}^{(SM)} + \mathcal{M}^{(Q)}|^2. \quad (7)$$

The total energy loss rate (\mathcal{Q}) or emissivity energy carried away by the neutrino pair per unit volume per unit time from the photo-neutrino process is given by [3, 4]

$$\begin{aligned} \mathcal{Q} &= \frac{1}{(2\pi)^{11}} \int \frac{d^3 p}{2E} \left[\frac{2}{\exp[(E - \mu_e)/k_B T] + 1} \right] \int \frac{d^3 k}{2\omega} \frac{2}{\exp[\omega/k_B T] - 1} \int \frac{d^3 p'}{2E'} \left[1 - \frac{1}{\exp[(E' - \mu_e)/k_B T] + 1} \right] \\ &\times (E + \omega - E') \int \frac{d^3 q_1}{2E_\nu} \int \frac{d^3 q_2}{2E_{\bar{\nu}}} (2\pi)^4 \delta^4(p + k - p' - q_1 - q_2) \frac{1}{4} \sum_{s, \epsilon} |\mathcal{M}_t|^2 \end{aligned} \quad (8)$$

where $p = (E, \vec{p})$, $p' = (E', \vec{p}')$, $k = (\omega, \vec{k})$, $q_1 = (E_\nu, \vec{q})$ and $q_2 = (E_{\bar{\nu}}, \vec{q}')$ are the four momentum of the incoming electron, the outgoing electron, the photon, the neutrino and the anti-neutrino, respectively. μ_e is the electron chemical potential, k_B is the Boltzmann constant and T is the Stellar temperature. The factor of 2 in front of the electron distribution function $f_e(E) = (\exp[(E - \mu_e)/k_B T] + 1)^{-1}$ and photon distribution function $f_\gamma(\omega) = (\exp[\omega/k_B T] - 1)^{-1}$ take in to account the two spin states of those particles, while the factor of $\frac{1}{4}$ corresponds to the average over initial spin states. In the sum, the index s indicates sums over electrons spin states, while ϵ indicates a sum over the photon spins. The factor $[1 - (\exp[(E' - \mu_e)/k_B T] + 1)^{-1}]$ accounts for the Pauli-blocking factor of outgoing electrons. The energy loss rate \mathcal{Q} in Eq. (8) cannot be calculated analytically for all temperature and chemical potential.

The sum of the photon polarization is carried in terms of its longitudinal and transverse components

$$\sum_{\lambda=1}^2 \epsilon^{\mu*} \epsilon^\nu = -g^{\mu\nu} + \frac{k^\mu k^\nu}{k^2} = P_{\mathcal{L}}^{\mu\nu} + P_{\mathcal{T}}^{\mu\nu}. \quad (9)$$

where longitudinal and transverse components are given as

$$P_{\mathcal{L}}^{\mu\nu} = \sum_{\lambda=1}^2 \epsilon^{\lambda\mu} \epsilon^{\lambda\nu} - P_{\mathcal{T}}^{\mu\nu} \quad (10)$$

$$P_{\mathcal{T}}^{\mu\nu} = \begin{cases} \delta^{ij} - \frac{k^i k^j}{k^2} & \text{for } i, j = 1, 2, 3 \\ 0 & \text{for } \mu \text{ or } \nu = 0. \end{cases} \quad (11)$$

The photon polarization tensor mentioned above perform the following features

$$P_{\mathcal{T}}^{\mu\beta} P_{\mathcal{L}\beta\nu} = 0, P_{\mathcal{L}}^{\mu\beta} P_{\mathcal{L}\beta\nu} = -P_{\mathcal{L}\nu}^\mu, P_{\mathcal{T}}^{\mu\beta} P_{\mathcal{T}\beta\nu} = -P_{\mathcal{T}\nu}^\mu, P_{\mathcal{L}\mu}^\mu = -1, P_{\mathcal{T}\mu}^\mu = -2.$$

By using these relations, one can write that the longitudinal (\mathcal{L}) and the transverse (\mathcal{T}) component of the squared total matrix elements as:

$$\sum_{s, \epsilon} |\mathcal{M}_t^{(\mathcal{L}, \mathcal{T})}|^2 = 32e^2 G_F^2 \left\{ (C'_V{}^2 - C_A^2) m_e^2 |\mathcal{M}_-^{(\mathcal{L}, \mathcal{T})}|^2 + (C'_V{}^2 + C_A^2) |\mathcal{M}_+^{(\mathcal{L}, \mathcal{T})}|^2 + C'_V C_A |\mathcal{M}_{+-}^{(\mathcal{L}, \mathcal{T})}|^2 \right\} \quad (12)$$

here we do not present the expressions $|\mathcal{M}_-^{(\mathcal{L},\mathcal{T})}|^2, |\mathcal{M}_+^{(\mathcal{L},\mathcal{T})}|^2, |\mathcal{M}_{+-}^{(\mathcal{L},\mathcal{T})}|^2$ because they are very long. Our calculation is parallel to the calculation done by Duttì et al. (one can see [11] for the details).

Performing integration momentum p and k , we get

$$I(p', q_1, q_2) = \frac{1}{\pi^2} \int \frac{d^3 p}{2E} \int \frac{d^3 k}{2\omega} f_\gamma(\omega) f_e(E) \delta^4(p+k-p'-q_1-q_2) \sum_{s,\epsilon} |\mathcal{M}_t^{(\mathcal{L},\mathcal{T})}|^2. \quad (13)$$

Then for the total energy loss we have

$$\mathcal{Q} = \frac{1}{(2\pi)^9} \int \frac{d^3 q_1}{2E_\nu} \int \frac{d^3 q_2}{2E_{\bar{\nu}}} \int \frac{d^3 p'}{2E'} [1 - f_e(E')] (E + \omega - E') I(p', q_1, q_2). \quad (14)$$

Denote the angle between $\vec{p} + \vec{k}$ and \vec{k} as θ_k , we obtain

$$I(p', q_1, q_2) = \frac{1}{4(2\pi)^2} \int_0^\infty \frac{|\vec{k}|}{\omega} d|\vec{k}| \int_0^{2\pi} d\varphi_k f_\gamma(\omega) f_e(E) \frac{1}{|\vec{p} + \vec{k}|} \sum_{s,\epsilon} |\mathcal{M}_t^{(\mathcal{L},\mathcal{T})}|^2. \quad (15)$$

Finally, for the differential energy loss from Eq. (14) we find

$$\frac{d^3 \mathcal{Q}}{dE_\nu dE_{\bar{\nu}} d(\cos\theta_{\nu\bar{\nu}})} = \frac{\pi^2}{(2\pi)^9} E_\nu E_{\bar{\nu}} \int_0^\infty \frac{|\vec{p}'|^2}{E'} d|\vec{p}'| \int_{-1}^1 d(\cos\theta_e) \int_0^{2\pi} d\phi_e [1 - f_e(E')] (E_\nu + E_{\bar{\nu}}) I(p', q_1, q_2). \quad (16)$$

In leading order, the dispersion relations of the photon in a plasma for the photo-neutrino process are

$$\omega_L^2 = \omega_P^2, \quad \omega_T^2 = \omega_P^2 + |\vec{k}|^2$$

where ω_P is the plasma frequency.

It is helpful to describe the foremost physical scales in the photo-neutrino production process of the neutrino pairs under limited circumstance for obtaining a qualitative and in many cases a quantitative understanding of the neutrino emissivity as a function of the temperature. We can procure the degenerate plasma which occurs in all temperature levels at sufficiently high densities, and a non-degenerate relativistic plasma that has high temperature but low density.

We will investigate the term \mathcal{Q}_T for transverse case; the analysis for the longitudinal case can be performed along the similar way. Although we cannot calculate the total energy loss rate analytically for all T and μ_e , we will consider for evaluating (\mathcal{Q}) in three different regions where it can be done analytically, namely, for nondegenerate, intermediate and degenerate electrons.

2.1 The Nondegenerate Case

This case occurs at enough low densities for which $\mu_e - m_e \ll T$. For $T \geq 10^{10} K$, the electron mass can be neglected in comparison to μ_e . In the relativistic case, the electron density and the plasma frequency are given as [37]

$$n_e = \frac{\mu_e}{3\pi^2} (\mu_e^2 + T^2 \pi^2) \simeq \frac{\mu_e T^2}{3}$$

$$\omega_P^2 = \frac{4\alpha}{3\pi} (\mu_e^2 + \frac{T^2 \pi^2}{3}) \simeq 4\pi\alpha \frac{T^2}{9}.$$

In this case both electron momentum and energy are of order of $E \simeq |\vec{p}| \simeq T$ and similarly both the photon momentum and energy are $\omega \simeq |\vec{k}| \simeq T$. So, we obtain for the squared total matrix element as

$$\sum_{s,\epsilon} |\mathcal{M}_t^T|^2 \simeq 256\pi\alpha G_F^2 (C_V'^2 + C_A'^2) E E_\nu E_{\bar{\nu}} / E'. \quad (17)$$

Then performing the phase space integration we have

$$\mathcal{Q}_T = \frac{20\alpha G_F^2 (C_V'^2 + C_A'^2)}{3(2\pi)^6} T^9 \int_0^\infty \frac{x^2 dx}{e^x + 1} \int_0^\infty \frac{y dy}{e^y - 1} \int_0^{x+y} \frac{(x+y-z)^3 dz}{e^{-z} + 1} \quad (18)$$

where $x \equiv E/T, y \equiv \omega/T$ and $z \equiv E'/T$. Analytical approximation to these integrals can be obtained by replacing $\frac{1}{e^{-z}+1} \rightarrow 1$. In this limit we find

$$\int_0^\infty \frac{x^2 dx}{e^x+1} \int_0^\infty \frac{y dy}{e^y-1} \int_0^{x+y} \frac{(x+y-z)^3 dz}{e^{-z}+1} = \frac{63}{256} \Gamma(7) \zeta(7) \Gamma(2) \zeta(2) + \frac{37}{22} \Gamma(6) \zeta(6) \Gamma(3) \zeta(3) + \frac{73}{32} \Gamma(5) \zeta(5) \Gamma(4) \zeta(4)$$

where $\Gamma(n)$ and $\zeta(n)$ are standard gamma and zeta functions, respectively.

In this limit, we obtain

$$\mathcal{Q}_T \simeq \frac{20042}{3(2\pi)^6} \alpha G_F^2 (C_V'^2 + C_A^2) T^9. \quad (19)$$

2.2 The Intermediate Case

In this case $\mu_e > T > \omega_p$, the energy loss rate \mathcal{Q}_T is strongly dependent on density. In this density range, the dominant energies are $E \simeq |\vec{p}| \simeq \mu_e, \omega \simeq |\vec{k}| \simeq T, E_\nu \simeq |\vec{q}| \simeq T$. With this energy scales the squared total matrix element is estimated as

$$\sum_{s,\epsilon} |\mathcal{M}_t^T|^2 \simeq 256\pi\alpha G_F^2 (C_V'^2 + C_A^2) \frac{1}{4\mu_e T \omega_p^2} T^4 \mu_e^2. \quad (20)$$

Similar to the nondegenerate case, the phase space integration brings

$$\mathcal{Q}_T \simeq \frac{32\alpha G_F^2 (C_V'^2 + C_A^2) T^9 \mu_e^2}{3(2\pi)^6 \omega_p^2} \zeta(5) \Gamma(5, \omega_p/T) \quad (21)$$

where $\Gamma(n, m)$ is the incomplete gamma function.

In the case of the maximum emissivity, the ratio $\frac{\omega_p}{T} \ll 1$, for energy loss rate we get

$$\mathcal{Q}_T \simeq \frac{768}{3(2\pi)^6} \alpha G_F^2 (C_V'^2 + C_A^2) \frac{T^9 \mu_e^2}{\omega_p^2} e^{-\omega_p/T}. \quad (22)$$

2.3 The Degenerate Case

As the last case, μ_e and $\omega_p \gg T$ and m_e where $\mu_e \simeq (3\pi^2 n_e)^{1/3}$, $\omega_p \simeq \sqrt{4\alpha/3\pi} \mu_e \simeq \mu_e/18$, one can obtain [37]

$$n_e = \frac{1}{\pi^2} \int_0^\infty dp p^2 \left[\left(\exp\left(\frac{E-\mu_e}{k_B T}\right) + 1 \right)^{-1} - \left(\exp\left(\frac{E'-\mu_e}{k_B T}\right) + 1 \right)^{-1} \right].$$

The Pauli blocking factor of outgoing electron provides that the electrons lie close to the Fermi surface. In this case electrons are elastically scattered exchanging only the 3-momentum with the photon and outgoing neutrinos. Under this circumstances, it is expected that both electron energies would be $E \simeq E' \simeq |\vec{p}| \simeq |\vec{p}'| \simeq \mu_e$. As a results, the photon's entire energy is converted to the neutrino-antineutrino pair energy. Hence the photon energy and momentum are $\omega \simeq \omega_p \simeq E_\nu + E_{\bar{\nu}}$ and $|\vec{k}| \simeq T, E_\nu \simeq |\vec{q}| \simeq \omega_p/2$. In this limit the squared matrix element can be approximated by

$$\sum_{s,\epsilon} |\mathcal{M}_t^T|^2 \simeq 16\pi\alpha G_F^2 (C_V'^2 + C_A^2) \omega_p^2. \quad (23)$$

Then energy loss rate becomes

$$\mathcal{Q}_T \simeq \frac{4\alpha G_F^2 (C_V'^2 + C_A^2)}{3(2\pi)^6} \omega_p^6 T^3 e^{-\omega_p/T}. \quad (24)$$

3 Numerical Results and Discussion

In this section, we will present our numerical results for the energy loss rate for considered three different cases in terms of tables and figures. For the numerical calculations we have selected the range for the neutrino charge radius $\langle r_\nu^2 \rangle$ as $[0, 100] \cdot 10^{-32} \text{cm}^2$ and for the temperature T as $[10^8 \text{K}, 10^{11} \text{K}]$ (see [18–21]).

Firstly, in Table 1, Table 2 and Table 3, we displayed the energy loss rate values ($\mathcal{Q}_T(\text{erg}/\text{cm}^3 \cdot \text{s})$) for all three cases for the different values of T and $\langle r_\nu^2 \rangle \cdot 10^{-32} \text{cm}^2$. It is seen that the charge radius contribution is considerable

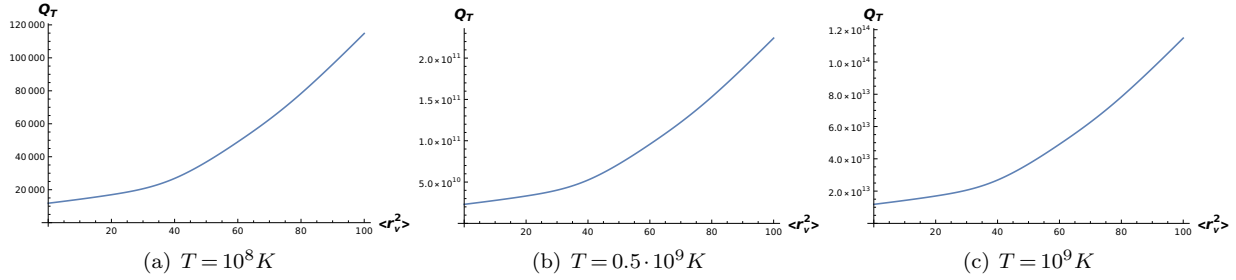
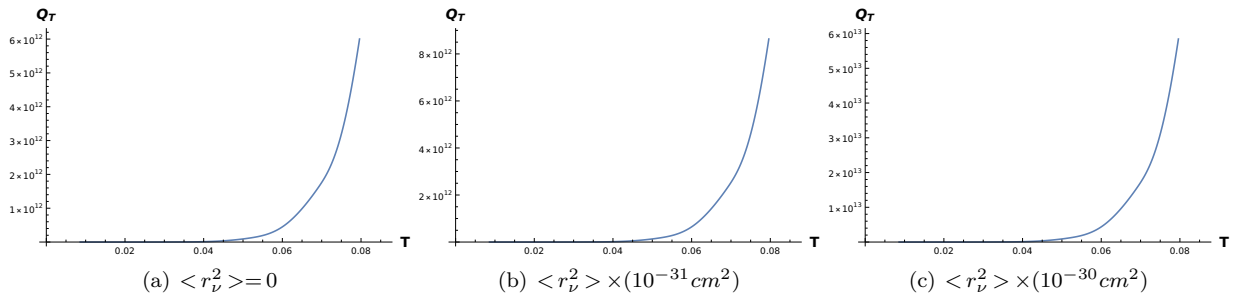
		$\langle r_\nu^2 \rangle \cdot 10^{-32} \text{cm}^2$			
		0	2.5	10	100
T	$10^8 K$	1.17908×10^4	1.29761×10^4	1.69596×10^4	1.14784×10^5
	$10^9 K$	1.17908×10^{13}	1.29761×10^{13}	1.69596×10^{13}	1.14784×10^{14}
	$10^{10} K$	1.17908×10^{22}	1.29761×10^{22}	1.69596×10^{22}	1.14784×10^{23}
	$10^{11} K$	1.17908×10^{31}	1.29761×10^{31}	1.69596×10^{31}	1.14784×10^{32}

 Table 1: Energy loss rate values ($Q_T(\text{erg}/\text{cm}^3 \cdot \text{s})$) for the nondegenerate case.

		$\langle r_\nu^2 \rangle \cdot 10^{-32} \text{cm}^2$			
		0	2.5	10	100
T	$10^8 K$	1.00253×10^5	1.10332×10^5	1.44202×10^5	9.75972×10^5
	$10^9 K$	1.00253×10^{14}	1.10332×10^{14}	1.44202×10^{14}	9.75972×10^{14}
	$10^{10} K$	1.00253×10^{23}	1.10332×10^{23}	1.44202×10^{23}	9.75972×10^{23}
	$10^{11} K$	1.00253×10^{32}	1.10332×10^{32}	1.44202×10^{32}	9.75972×10^{32}

 Table 2: Energy loss rate values ($Q_T(\text{erg}/\text{cm}^3 \cdot \text{s})$) for the intermediate case.

		$\langle r_\nu^2 \rangle \cdot 10^{-32} \text{cm}^2$			
		0	2.5	10	100
T	$10^{10} K$	2.60048×10^{20}	2.8619×10^{20}	3.74047×10^{20}	2.53158×10^{20}
	$3 \times 10^{10} K$	5.11852×10^{24}	5.63309×10^{24}	7.36237×10^{24}	4.98292×10^{25}
	$5 \times 10^{10} K$	5.07906×10^{26}	5.58966×10^{26}	7.30561×10^{26}	4.9445×10^{27}
	$10 \times 10^{10} K$	2.60048×10^{29}	2.8619×10^{29}	3.74047×10^{29}	2.53158×10^{32}

 Table 3: Energy loss rate values ($Q_T(\text{erg}/\text{cm}^3 \cdot \text{s})$) for the degenerate case.

 Fig. 2: Energy loss rate values ($Q_T(\text{erg}/\text{cm}^3 \cdot \text{s})$) versus charge radius ($\langle r_\nu^2 \rangle \times (10^{-32} \text{cm}^2)$) for different values of the temperature (T) for the nondegenerate case.

 Fig. 3: Energy loss rate values ($Q_T(\text{erg}/\text{cm}^3 \cdot \text{s})$) versus temperature ($T(10^9 K)$) for different values of the charge radius ($\langle r_\nu^2 \rangle$) for the nondegenerate case.

at high temperature in all considered cases. Also, one can observe that there is an effective change in the energy loss

rate for the degenerate case compared to the other one.

In Figure 2 and Figure 3 we visualized the effect of T and $\langle r_\nu^2 \rangle \times (10^{-32} \text{cm}^2)$ on the energy loss rate values ($Q_\tau(\text{erg}/\text{cm}^3 \cdot \text{s})$). As expected from the obtained formulas, the change with respect to T is more stronger compared to change with respect to $\langle r_\nu^2 \rangle$.

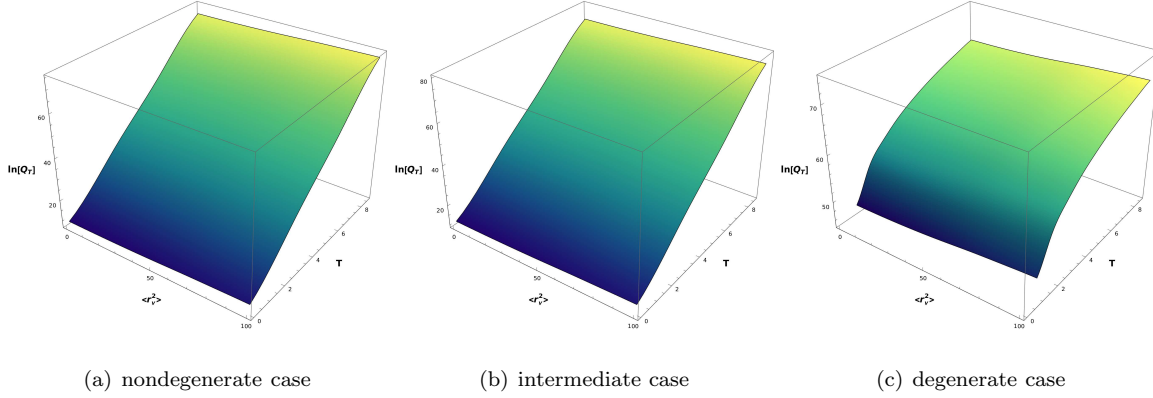


Fig. 4: Logarithm of the total energy loss rate values ($\ln(Q_\tau(\text{erg}/\text{cm}^3 \cdot \text{s}))$) versus charge radius and temperature ($T(10^9 \text{K})$) for the $\langle r_\nu^2 \rangle \times (10^{-32} \text{cm}^2)$ in (a) and $\langle r_\nu^2 \rangle \times (10^{-30} \text{cm}^2)$ in (b) and (c).

Finally, in Figures (4) we plotted the 3-D graph of $\ln(Q_\tau)$ for the values of temperature and charge radius. Similar to the table results, it is seen that the change in the the total energy loss rate is different in the degenerate case compared to the two other cases due to the division energy of the photon by the neutrino and anti-neutrino.

4 Conclusion

As a conclusion, in this study we have calculated energy loss rate of photo-neutrino process, considering neutrino charge radius (or anapole moment) effects. It is obtained that, the contribution for the charge radius change the result about $\sim 10\%$. The neutrinos' magnetic moment contribution is very small. We observed that if the neutrino magnetic moment have $\mu_\nu = 10^{-6} \mu_B$ order, then the effect of the indicated term becomes dominant and the contribution should be taken under consideration. However, this value is still bigger than the tau-neutrino's magnetic moment.

References

- 1 Ritus VI 1962 *Zh. Eksp. Thor. Fiz.* **41** 1285; *Sov.Phys.JTEP* **14** 915
- 2 Chiu H-Y and Stabler RC 1962 *Phys. Rev.* **122** 1317
- 3 Beaudt G, Petrosian V and Salpeter EE 1966 *Phys. Rev.* **154** 1445
- 4 Beaudt G, Petrosian V and Salpeter EE 1967 *Astrophys. J.* **150** 979
- 5 Dicus DA 1972 *Phys. Rev. D* **6** 941 (1972).
- 6 Schinder PJ, Schramm DN, Wiita PJ, Margolis SH and Tubbs DL 1987 *Astrophys. J.* **313** 531
- 7 Itoh N, Adachi T, Nakagawa M, Kohyama Y and Munakata H 1989 *Astrophys. J.* **339** 354
- 8 Munakata H, Kohyama Y and Itoh N 1985 *Astrophys. J.* **296** 197
- 9 Aydemir A, Aydin C and Sever R 2001 *Modern Phys. Lett. A* **16** 497
- 10 Bhattacharyya I, *arXiv:1510.02678 [physics.gen-ph]*
- 11 Dutta SI, Ratkovic S and Prakash M 2004 *Phys. Rev. D* **69** 023005
- 12 Prakash M, S. Ratkovic S and S.I. Dutta SI 2003 *KLAS-APCTP Inter.Sym.in Astro-Hadron Phys.;* *Compact Stars* **476**
- 13 Barut AO, Aydin ZZ and Duru IH 1985 *Phys. Rev. D* **32** 3051
- 14 Lenard A 1953 *Phys.Rev.* **90** 968
- 15 Aydin C 2022 *Chinese Phys. C* **46** 073107
- 16 Aydin C *Mod.Phys. Lett. A* (submitted)
- 17 Aydin C *arXiv: 1910.09545 [hep-ph]*
- 18 Khan AN 2019 *J. Phys. G. Nucl. Part. Phys.* **46** 035005
- 19 Khan AN 2020 *Phys. Lett. B* **809** 135782
- 20 Khan AN 2021 *Phys. Lett. B* **819** 136415
- 21 Khan AN *arXiv:2203.08892(hep-ph)*
- 22 Kayser B and Goldhaber AS 1983 *Phys. Rev. D* **28** 2341
- 23 Giunti C and Studenikin A 2015 *Rev. Mod. Phys.* **87** 531
- 24 Bernabe J, Papavassiliou J and Vidal J 2004 *Nucl.Phys. B* **680** 450
- 25 Kerimov BK, Zeinalov SM, Alizade VN and Mourao V 1992 *Phys. Lett. B* **274** 477
- 26 Dvornikov M and Studenikin A 2004 *Phys. Rev. D* **69** 073001

- 27 Guinti C, Kouzakov KA, Li Y-F, Lokhov AV, Studenikin AI and Zhou S 2016 *Ann. Phys.* **528** 198
- 28 Kouzakov KA and Studenikin AI 2017 *Phys. Rev. D* **95** 055013
- 29 Cadeddu M, Guinti C, Kouzakov KA, Li Y-F, Studenikin AI and Zhang YY 2018 *Phys. Rev. D* **98** 113010
- 30 Vogel P and Engel J 1989 *Phys. Rev. D* **39** 2278
- 31 Barranco J, Miranda OG and Rashba TI 2008 *Phys. Lett. B* **662** 431
- 32 Hutaaruk PTP, Oh C and Tsushima K 2018 *Phys. Rev. D* **98** 013009
- 33 Hutaaruk PTP, Sulaksono A and Tsushima K 2022 *Nucl. Phys. A* **1017** 122356
- 34 Bell NF, Cirigliano V, Ramsey-Musolf MJ, Vogel P and Wise MB 2005 *Phys. Rev. Lett.* **95** 151802
- 35 Capozzi F and Raffelt G 2020 *Phys. Rev. D* **102** 083007
- 36 Gninenko SN and Krasnikov NV 2000 *Phys. Lett. B* **490** (1-2) 9
- 37 Braaten E and Segel D 1993 *Phys. Rev. D* **48** 1478